The Promising of Tiles as Barrier on DBD with Narrow Gap and Produced Ozone

Fri Murdiya, Ericko Hardiwika, Muhammad Rafi Epafras, Faisal Setiawan, Firdaus, Amir Hamzah, Febrizal

Dept. Electrical Engineering, Universitas Riau, Pekanbaru, Indonesia
Jl. HR Subrantas KM 12,5 Panam, Pekanbaru, Indonesia

Abstract: The high voltage plasma that occurs in the air gap and in the dielectric barrier discharge (DBD) is caused by the high voltage stress the gas molecules to ionized gas molecules. DBD is also determined by the type of barrier made of materials with various dielectric constants. The power supply used in this study is a parallel resonant pushpull inverter using a flyback transformer. Five types of ceramics (K1, K2, K3, K4, and K5) and two types of granites (G1 and G2) as barriers were used in this study. The gap between the high voltage electrode and the barrier was 1.2 mm. The results showed that plasma with high light intensity is found in K3, K5, G1 and G2. Discharge current in G1 is higher than others. The highest discharge voltage occurs in the G1 with an air gap of 1.2 mm. K3, K5, K1 and K2 have better ozone concentrations than K1, K2 and K4. From the results of the calculation of the dielectrics used, all of them have a dielectric permittivity value of less than 15 and the relative permittivity of these ceramics affects the shape of the plasma, the light intensity of the plasma and the concentration of ozone produced. This type of granite as barrier that produces light intensity, plasma voltage, discharge current and the resulting ozone concentration is higher than the ceramic type.

Keyword: DBD, ceramics, granite, plasma intensity, voltage and current, ozone

1. Introduction

Non-thermal plasma at atmospheric pressure by the dielectric barrier discharge (DBD) method has become a promising tool for several fields of scientific research and practical applications, such as electro aerodynamic propulsion, ozone synthesis, plasma catalysis, cancer treatment and others [1-4]. DBD is often used as a source of non-thermal plasma because it allows the generation of non-thermal plasma that is evenly distributed across the barrier at atmospheric pressure in an easier way. In addition, it is easier for researchers to design DBD in many geometries and can easily improve their performance [5]. The DBD reactor is made with an arrangement of two electrodes separated by one or more dielectric layers [6]. Several reactor geometries have been investigated in recent decades [7]. More complex arrangements appear in the two dimensions of DBD [8] including squares, hexagons and others [9-11]. DBD is an electric discharge process in a layered dielectric system between air dielectric and a solid dielectric which is connected with a high voltage power supply where plasma is formed in the air dielectric because the electric field strength of the air dielectric is higher than the solid dielectric, so that gas molecules (O_2, CO, CO_2, N_2, NO_x, etc.) in the air dielectric easier to ionize or deionize. There are several types of DBD as shown in Figure 1.

Preliminary results in [12] show that DBD connected to a high-voltage source with unipolar symmetrical pulses behaves similarly to sinusoidally operated DBD. Unipolar-pulsed-driven DBD exhibits a single micro-discharge (MD) during the rise and fall of the voltage pulse, that is, also when the potential at the electrode is changed to zero without changing the sign of the polarity at the electrode. MD appears in every half period of the applied voltage while the potential of the driven electrode changes. Thus, the emergence of MD in the new half-period is also induced by field reversal. From this point of view, a comparison between pulse-driven and sinusoidal DBD needs to be made with a bipolar applied voltage, which represents the same type of potential change but at a different voltage. A number of papers in the literature have compared

Received: October 27th, 2021. Accepted: March 2nd, 2022
DOI: 10.15676/ijeei.2022.14.1.2

pulsed and sinusoidal high-voltage sources as in refs [13, 14]. Experiments with a single MD as the basis for a multi-filament system have been reported. In the case of pulse-driven operation, this has so far not received much attention in the literature. Experimental details include spatially dependent streamer speed, single MD image, high resolution voltage and current curves, and transferred charge values.

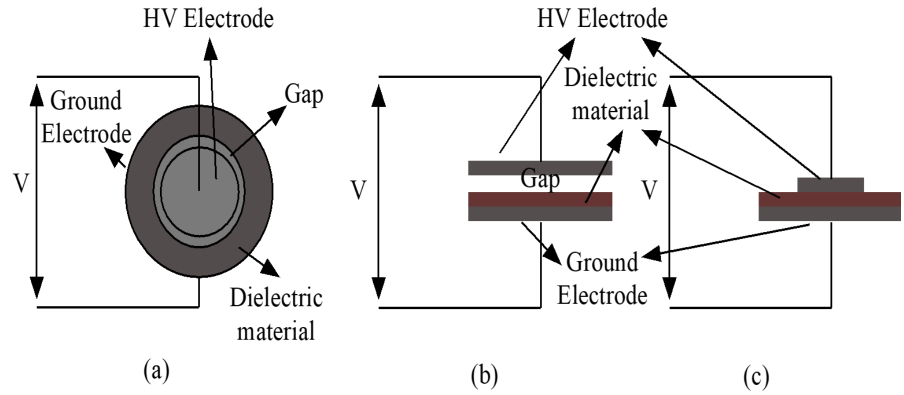

Figure 1. Dielectric barrier discharge arrangement. (a). Cylindrical DBD, (b) Planar DBD, (c) Surface DBD.

The barrier used as an insulating layer is glass, quartz, ceramic, and a polymer layer as an insulating layer. The type of material, thickness and surface structure of the dielectric material can affect the plasma discharge. DBD is generally used as a method of generating high-voltage ozone, also known as a high-voltage plasma generator. High-voltage plasma generators are widely used in various areas such as medicine, chemistry and physics. This technology consists of a high-voltage generator, electrodes and a dielectric part. How it works is by supplying the dielectric barrier discharge with a high voltage which at a certain value will produce a plasma that is visible to the eye. This plasma occurs due to the failure of a material to maintain its insulating properties [15,16]. Ozone is a gas that is widely used in various fields, for example it is used as a disinfectant for water treatment, sterilization of medical devices and food preservation. Ozone is an almost colorless gas with a characteristic odor and can be detected by humans at low concentrations of 0.01 ppm. This ozone can be produced by the dielectric barrier discharge method, which is generally used as an ozone generation method supplied by sinusoidal and non-sinusoidal high voltages. In this study, several floor tiles and granite were tested such as permittivity, plasma light intensity, discharge current and voltage and ozone concentration. Ceramics and granite were chosen as DBD in this study because not many scientists had investigated their electrical properties. Ceramics and granite are also easier to find in the market and are cheaper.

2. Experimental procedures

A. High voltage generator circuit and experiment set up

The use of a high-voltage resonant inverter in an ozone generator with a full push configuration has been reported [16]. The function of the parallel resonant push-pull inverter is to generate an alternating current with a frequency in the order of kiloHertz, so that, the voltage can be increased by using a fly-back transformer which requires input voltage in the order of kiloHertz. This construction is smaller than the high voltage transformer which is supplied with an alternating current of 50 Hz frequency. Parallel switch (MOSFET) was chosen because the results of previous studies found damage to the MOSFET repeatedly. So that this circuit is also added a current sensor connected to the microcontroller to detect overcurrent which can damage the circuit. The complete electronic circuit of the resonant inverter is given in Figure 2. The input voltage of the inverter was supplied from a direct current (DC) power supply of 15 volts. The ignition side of this inverter was installed with IC CD4047, an integrated PWM (pulse width modulation) circuit. Six MOSFETs (M1…M6) were connected in parallel to form a bridge and mounted to 12 Vdc. This circuit was equipped with an inductor (L) 10mH and connected in series with a capacitor (C2) 150nF. The output of the resonant circuit was connected to the low-voltage side of the fly-back transformer, with the primary winding being a center tap with multiple 10/2 windings. The high voltage resonant inverter generator was energized by an input voltage of 220VAC and a frequency of 50 Hz. The output voltage of this inverter can reach 8 kV under load conditions at a frequency of 20 kHz [16]. Measurement of the capacitance of each tile was using an LCR meter.

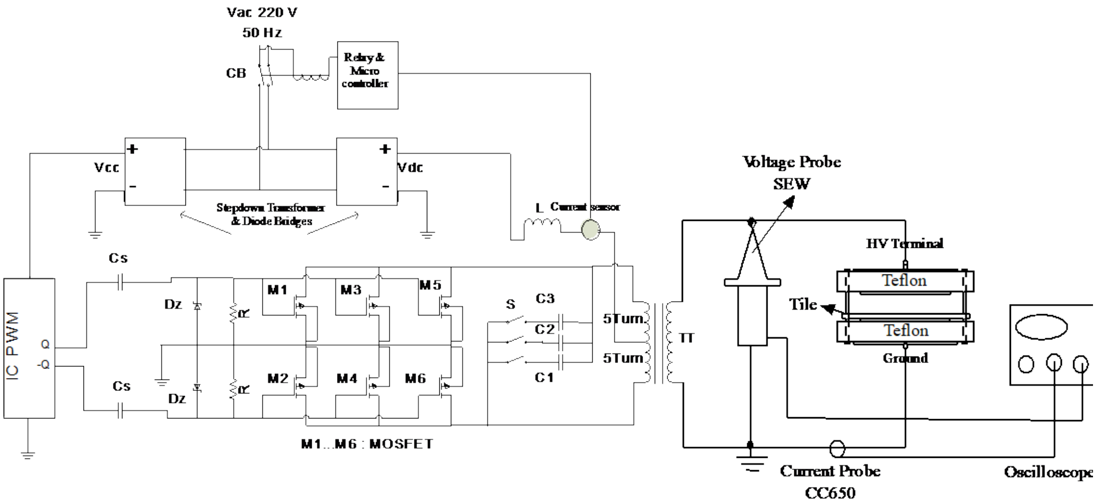

IC PWM: CD4047;
M1…M6: MOSFET IRFZ44N; L: Inductor (10 mH);
C1...C3: Capacitors (100 nF, 150 nF, 200 nF); Dz: Zener diode;
S: Switch
Cs: PWM Capacitor of 100 nF;
R: Resistor of 100 Ohm;

Figure 2. The electrical circuit for high voltage generation.

The tiles used were K1 to K5 and granite types G1 and G2 which are shown in Figure 2. Dielectric barrier discharge (DBD) was composed of high voltage and ground electrodes made of stainless steel. Bonding electrodes was using Teflon and bolt and nut was used as a spacer between the electrode gap and the barrier/tile. There were five types of floor tiles and two types of granite were used in this study. The image and shape of the ceramic is given in Figure 3. The distance between the hv electrode and the barrier was 1.2 mm. The light intensity of the plasma was recorded by the Aspectramini application on the android software. The discharge current and voltage were measured with a Hantek CC650 current probe and a SEW voltage divider with a ratio of 1,000:1. These discharge currents and voltages were recorded by a Hantek digital oscilloscope. The ozone produced by this ozone generator was measured using an HT-O3 Ozone meter. Ozone generator and production tests were carried out for all K1 to K5 and G1 and G2 dielectrics. This test was carried out at room temperature and a pressure of 1 atm.

Figure 3. Type of ceramics and granites.

3. Results and discussion

A. Values of Capacitance and Relative Permittivity for Sample Ceramics

Seven types of ceramic brands (tile K 1 to K5) and 2 types of granite (granite G 1 and G2) that installed as a barrier in an ozone generator were tested in this study. The measurement of the capacitance value without ceramics and the measurement of capacitance with ceramics was carried out using a measuring instrument, namely the LCR meter. From the results of the air capacitance measurement, the gap between the plates used as electrodes is as thick as ceramic, from five kinds of ceramics there are three different sizes of ceramics and two kinds of granite have the same thickness. The thickness of the ceramics is 8 mm (K1), 6 mm (K2, and K5), 7 mm (K3 and K4), and the thickness of two types of granite (G1 and G2) is 9 mm, respectively. From the results of the air capacitance measurement, the highest measurement value is at a frequency of 100 Hz with a ceramic thickness of 6 mm, which is 34 pF, and the lowest measurement results are at a frequency of 100 kHz with a thickness of G1 mm, which is 21.21 pF, respectively. The capacitance measurement value without ceramic is smaller than with the ceramic. From the results of measuring the capacitance of five kinds of ceramics and two kinds of granite using five different frequencies on the measuring instrument, it can be seen that the highest ceramic capacitance measurement value is at a frequency of 100 Hz, which is 252 pF at K5, the lowest ceramic capacitance value is at a frequency of 100 kHz, which is 95 pF in K1, the highest granite capacitance value is at a frequency of 100 Hz, which is 77 pF in G1 and the lowest granite capacitance value is at a frequency of 100 kHz, which is 50.29 in G2, respectively. The highest relative permittivity of ceramics is found in K3 and K5 with relative permittivity values of each with a measuring instrument frequency of 100 Hz, namely 7.41 and 7.61, respectively and G1 and G2 with relative permittivity values respectively with a measuring instrument frequency of

100 Hz, namely 4.52 and 5.83 respectively. The capacitance value of all ceramics is given in Figure 4. The highest capacitance in this experiment was obtained in ceramics of K5 at the testing frequency of 100 Hz, and the lowest value was ceramics of G2 which was a type of granite. In Figure 4, it can be seen that the capacitance decreases with increasing the testing frequency. However, the granite type of ceramics shows a more stable value for all testing frequencies. The relative permittivity of all ceramics is given in Figure 5. The ceramics of K1 to K5 shows that the relative permittivity decreases by increasing the test frequency. While in granite ceramics of G1 and G2, the relative permittivity slightly increases by increasing the frequency. This relative permittivity value affects the shape of the plasma or the value of the plasma light produced during the test. We can also look the plasma that occurs when each ceramic is used as a barrier in an ozone generator. This test was also carried out on DBD with the same air gap space.

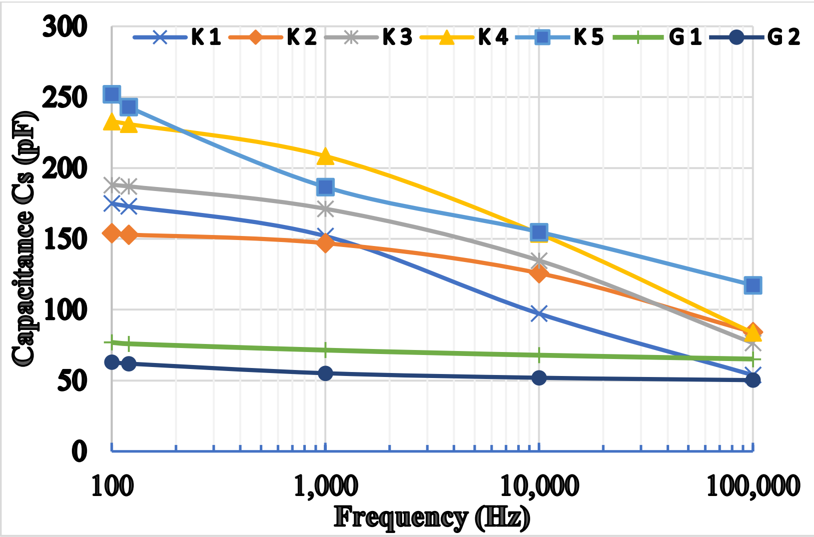

Figure 4. Capacitance of several tiles.

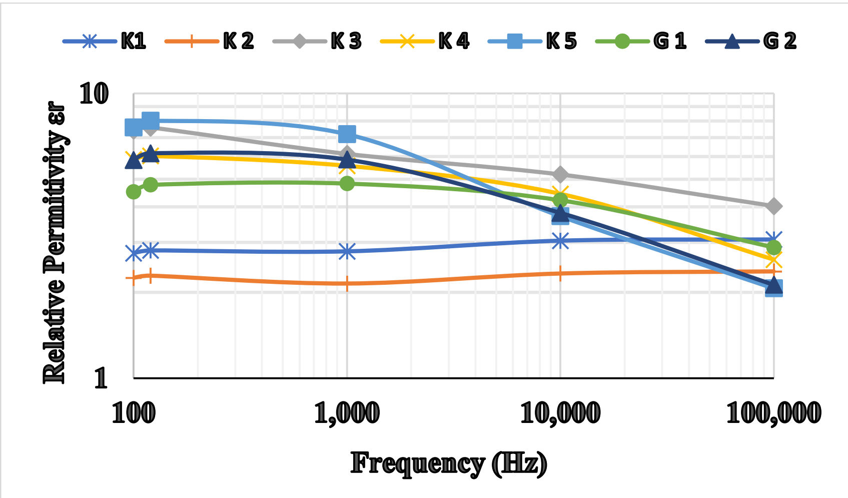

Figure 5. Relative permittivity of several tiles.

B. Plasma Light Intensity

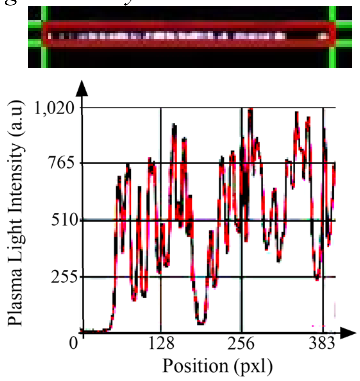

(a) Ceramic of K1

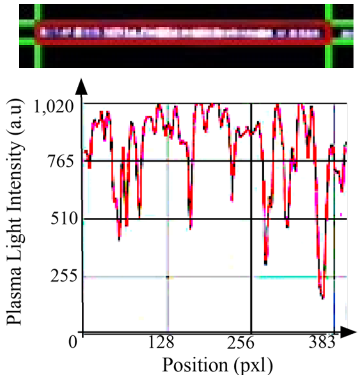

(b) Ceramic of K2

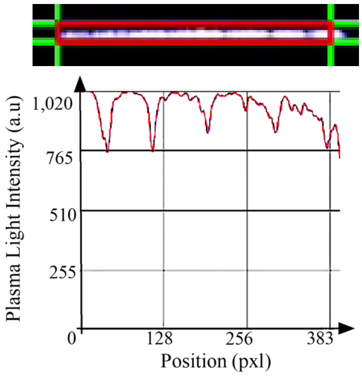

(c) Ceramic of K3

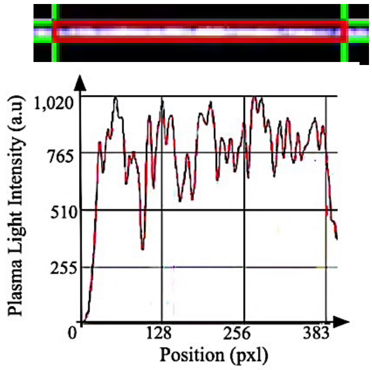

(d) Ceramic of K4

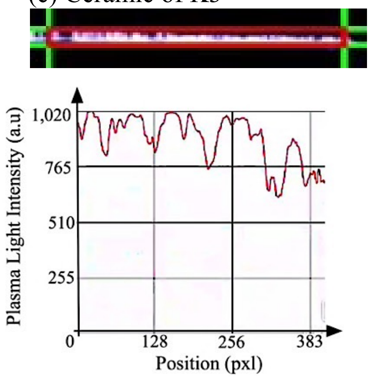

(e) Ceramic of K5

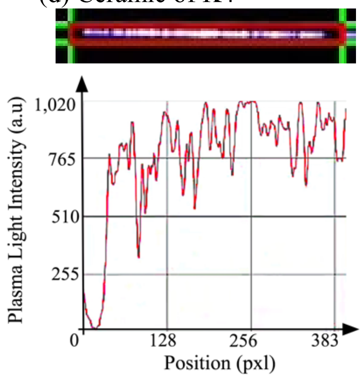

(f) Granite of G1

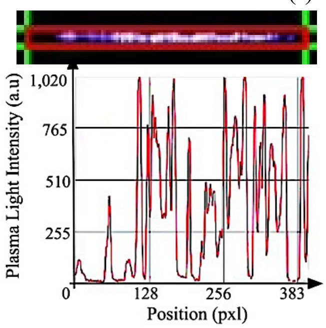

(g) Granite of G2

Figure 6. Plasma light intensity for several tiles

The results of using the AspectraMini application are in black/dark conditions, in this condition the light intensity value that is read will approach 0 (zero) a.u. While the results are in white/bright conditions, in this condition the light intensity value is at the point of 1.020 a.u. K1 used has a thickness of 8 mm and has ceramic permittivity values (Ɛr) with frequencies of 100 Hz, 120 Hz, 1 kHz, 10 kHz and 100 kHz are 2.75, 2.81, 2.79, 3.04 and 3.07, respectively. Figure 6(a) shows light intensities that vary from 40 a.u to 1020 a.u. At positions 0 to 383 pxl it can be seen that the plasma light intensity fluctuates and reaches its peak at a position of 270 pxl. This variation indicates that the plasma emission is not uniform. It is clear that K1 produces an inhomogeneous plasma. The ceramic of K2 used have a thickness of 6 mm and have ceramic permittivity values (Ɛr) with frequencies of 100 Hz, 120 Hz, 1 kHz, 10 kHz and 100 kHz are 2.25, 2.29, 2.15, 2.33 , and 2.37, respectively. Figure 6(b) presents varying plasma light intensities. At the pixel position 0 to 198, it can be seen that the plasma light intensity tends to fluctuate from 170 a.u to 1020 a.u in the 0 to 383 pxl position. The intensity of light tends to vary homogeneously. The ceramic of K3 used have a thickness of 7 mm and have ceramic permittivity values (Ɛr) with frequencies of 100 Hz, 120 Hz, 1 kHz, 10 kHz and 100 kHz are 7.41, 7.59, 6.13, 5.19, and 4.02, respectively. Figure 6(c) gives the plasma light intensity ranging from 765 a.u to 1020 a.u. It can be seen that the plasma light intensity for all positions 0 to 383 pxl fluctuates and is unstable. It is seen that the plasma light intensity is not homogeneous and shows that the plasma that occurs in the air gap is not uniform. The ceramic of K4 used has a thickness of 7 mm and has ceramic permittivity values (Ɛr) with frequencies of 100 Hz, 120 Hz, 1 kHz, 10 kHz and 100 kHz are 5.87, 6.03, 5.57, 4.44, and 2.61, respectively. Figure 6(d) shows that the plasma light intensity at positions 0 to 383 varies from 320 a.u to 1020 a.u and tends to be unstable. The ceramic of K5 used has a thickness of 6 mm and has ceramic permittivity values (Ɛr) with frequencies of 100 Hz, 120 Hz, 1 kHz, 10 kHz and 100 kHz are 7.61, 8.03, 7.2, 3.71, and 2.07, respectively. Figure 6(e) shows that the plasma light intensity at positions 0 to 198 pixels tends to be stable with intensity variations from 765 a.u to 1020. However, at 198 to 383 pxl, the plasma light intensity tends to decrease at the 310 pxl position. The granites of G1 used has a thickness of 9 mm and has ceramic permittivity values (Ɛr) with frequencies of 100 Hz, 120 Hz, 1 kHz, 10 kHz and 100 kHz are 4.52, 4.78, 4.83, 4.22, and 2.88, respectively. Figure 6(f) shows that the plasma light intensity at positions 0 to 383 pixels tends to be unstable with light intensity from 285 a.u to 1020 a.u. The granite of G2 used has a thickness of 9 mm and has ceramic permittivity values (Ɛr) with frequencies of 100 Hz, 120 Hz, 1 kHz, 10 kHz and 100 kHz are 5.83, 6.17, 5.86, 3.81, and 2.13, respectively. Figure 6(g) shows that the plasma light intensity at positions 0 to 383 pxl tends to be unstable with variations in plasma light intensity from 10 a.u to 1020 a.u.

The light intensity of the plasma formed in Figures 5a and 5g is the first type, and the second type in Figures 5b, 5d and 5f and the third type in Figures 5c and 5e occurs because the density of the plasma formed is similar and different. It can be concluded that the plasma density is influenced by the content of ionized and deionized gas molecules that make up the plasma. In addition, the plasma formed is also influenced by the chamber terminal voltage and the dielectric permittivity. It is indicated that the primary and secondary electrons movement to the barrier above the high voltage electrode, ionizing the gas and generating electron avalanches [17], [18]. It is known that the light intensity is proportional to the electron density, meaning that the light intensity increases from the ground electrode to the high voltage electrode with a maximum in the high voltage region where the electron density is maximum [19].

C. The voltages and displacement currents

Figure 7 presents the discharge currents and voltages for all types of tiles. The characteristics of the discharge current and voltage as shown in Figure 7(a). There are small noises in the discharge current. These noises occur in the negative cycle of the current waveform and there are less noises in the positive cycle of the current waveform. Furthermore, the highest noise occurs during the positive cycle. The peak voltage and discharge current for ceramic of K1 are 5.07 kV and 29.8 mA, respectively. Then, the discharge current and voltage as shown in Figure

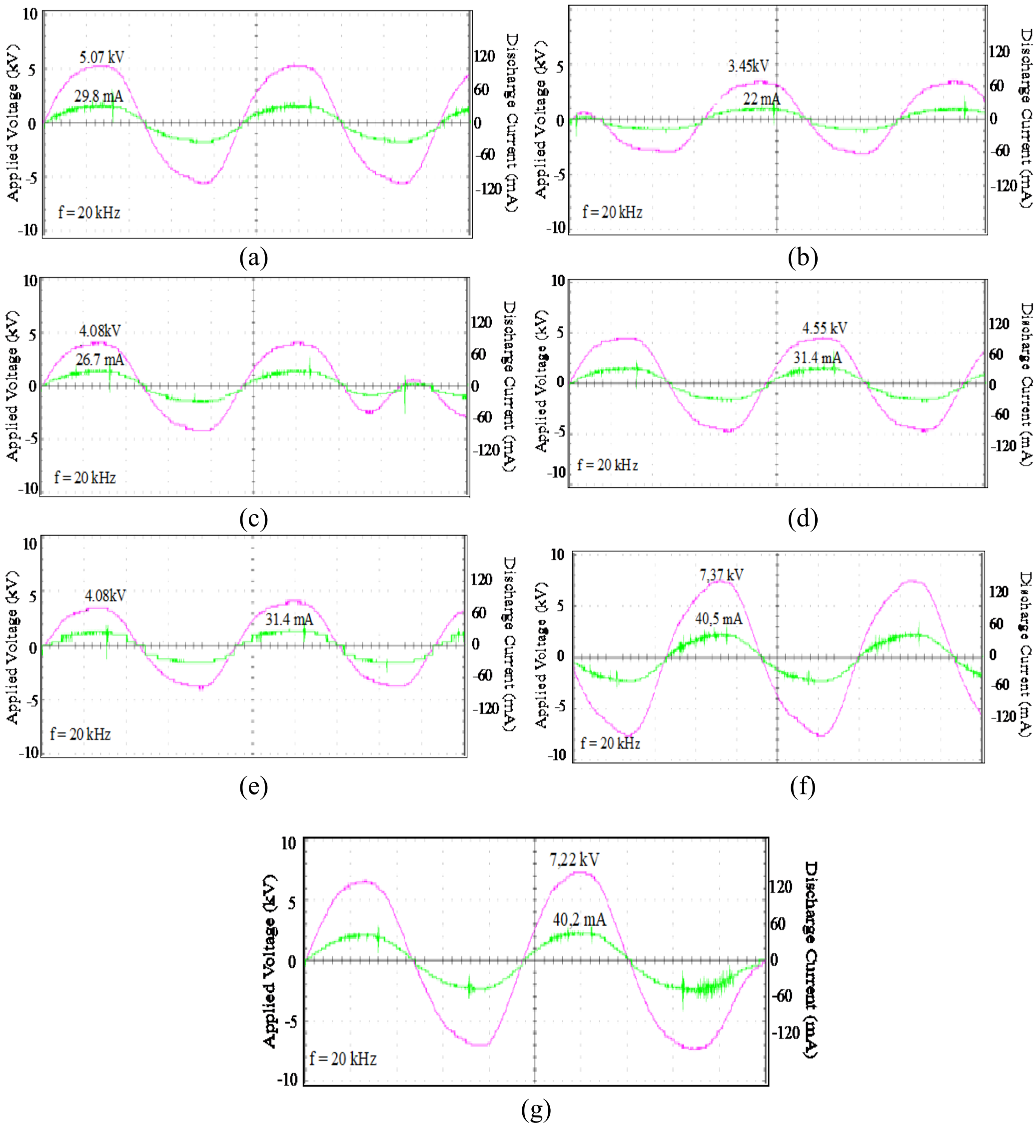

Figure 7. The voltages and displacement currents for several tiles. (a) Ceramic of K1, (b) ceramic of K2, (c) ceramic of K3, (d) ceramic of K4, (e) ceramic of K5, (f) granite of G1, and (g) granite of G2

7(b) shows that there are also small noises in the negative cycle of the current waveform and a lot of small noise in the positive cycle of the current waveform. This noise reaches its peak when the current waveform is in the positive cycle at the position of this wave near the zero value. The peak voltage and peak current for ceramic of K2 are 3.45 and 22mA, respectively. DBD with barrier as ceramic of K3 produces the voltage and discharge current as shown in Figure 7(c). There are small noises in the current waveform in both the negative cycle and a lot of noise in the positive cycle. This noise reaches its peak value around the maximum value of the discharge current. Peak voltage and current were reached at 4.08 kV and 26.7 mA, respectively. This is also found in Figure 7(d) for DBD with K4 as barrier. The peak values of the voltage and current are 4.55 kV and 31.4 mA, respectively. The noises that formed during the positive cycle of the current wave are more than the negative cycle. Noise reaches its peak value around the peak value of the discharge current. Figure 7(e) gives the values of the discharge voltage and current.

Peak values for voltage and current are reached at 4.08 kV and 31.4 mA, respectively. Noises are formed in the current waveform during both the positive and negative cycles. The current noises in the positive cycle are more than the negative cycle. The peak value of this noise occurs around the peak value of the discharge current. Figure 7(f) shows the value of voltage and current in DBD with barrier G1. The current noises that formed in the positive cycle of the current wave are more than the negative cycle. These noises occur when the current value is zero to its peak value. While the noises that formed on the current wave in the negative cycle are formed when the current wave is zero until it reaches its minimum value. The peak voltage and discharge current values for this DBD are 7.37 kV and 40.5 mA, respectively. Figure 7 (g) shows DBD with barrier G2 with peak voltage and current values of 7.22 kV and 40.2 mA, respectively. The noises that occur in the current wave during the positive cycle are less than the negative cycle. The noises during the positive cycle occur around the peak value of the discharge current and the peak value of the noise that rises in the negative cycle of the discharge current occurs around its minimum value. The peak voltage for DBD with barrier G1 is higher than for other barriers. Meanwhile, the highest peak current occurs in DBD with barrier G1 as well. This shows that the current and voltage in DBD are influenced by the type of barrier used. Noise formed on all tiles indicates that in the DBD gap there are a lot of micro discharges that cause the gas molecules to be ionized and most likely to form ozone.

The discharge current occurs continuously, and the gap voltage during gas breakdown extends. The plasma light intensity in Figure 6 shows a strong intensity on the barrier surface above the high-voltage electrode, and a weak luminosity appears on the barrier surface above the ground electrode [20][21].

D. Ozone Production

Measurement of ozone concentration was carried out using HT-E-O3. The unit of measurement for measuring ozone concentration is ppm (parts per million). This meter is capable of measuring the concentration of ozone produced up to 225 ppm. When measuring the ozone concentration, an air compressor is needed that functions so that the air pressure does not spread when the test is carried out. This air compressor is located in the shut-off valve and must be equal or in line with the gap or distance in the ozone generator. The measurements were made only at the best distance for each ceramic and granite dielectric, which was 1.2 mm. This test is carried out for 30 seconds. From the results of measuring the ozone concentration of ceramic 1 at a distance of 1.2 mm, the highest measurement value is 197.6 ppm/30 seconds. From the results of the measurement of the ceramic ozone concentration 2 at a distance of 1 mm, the highest measurement value is 155.1 ppm/30 seconds. Ceramic 5 is one of the best plasma producing dielectrics compared to other dielectrics. This can be seen from the results of measurements of ozone concentrations that have been carried out. Ozone concentration at a distance of 1.2 mm was 225 ppm at the 17th second. Granite 1 is one of the best plasma-producing dielectrics compared to other dielectrics. This can be seen from the results of measurements of ozone concentrations that have been carried out. Ozone concentration at a distance of 1.2 mm was 225 ppm at 15 seconds. Granite 2 is also one of the best plasma-producing dielectrics compared to other dielectrics. This can be seen from the results of measurements of ozone concentrations that have been carried out. Ozone concentration at a distance of 1.2 mm obtained 225 ppm in the 15th second. From the measurement of ozone concentration, the measurement results show that the best ozone concentration measurement results are found in the K3, K5, G1 and G2 dielectrics at a distance of 1.2 mm. The best measurement results can not be separated from the influence of the shape of the plasma and the intensity of the light produced. The better the shape of the plasma and the intensity of the light produced, the higher the concentration of ozone produced. Comparison of the measurement results of ozone concentration can be seen in the following Figure 8.

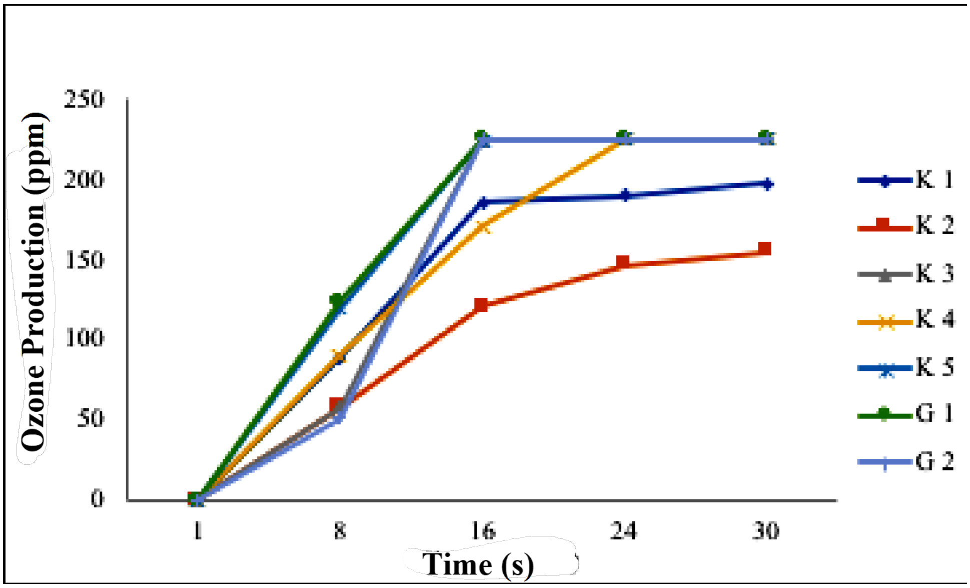

Figure 8. Ozone concentration measurement for several types of tile with gap Distance 1.2 mm

4. Conclusions

The results showed that plasma with high light intensity is found in K3, K5, G1 and G2. Discharge current in G1 is higher than others. The highest discharge voltage occurs in the G1 with an air gap of 1.2 mm. K3, K5, K1 and K2 have better ozone concentrations than K1, K2 and K4, respectively. Meanwhile, the highest peak current occurs in DBD with barrier G1 as well. This shows that the current and voltage in DBD are influenced by the type of barrier used. Noise formed on all tiles indicates that in the DBD gap there are a lot of micro discharges that cause the gas molecules to be ionized and most likely to form ozone. The measurement results show that the best ozone concentration measurement results are found in the K3, K5, G1 and G2 dielectrics at a distance of 1.2 mm. The best measurement results can not be separated from the influence of the shape of the plasma and the intensity of the light produced. The better the shape of the plasma and the intensity of the light produced, the higher the concentration of ozone produced. From the results of the calculation of the dielectrics used, all of them have a dielectric permittivity value of less than 15 and the relative permittivity of these ceramics affects the shape of the plasma, the light intensity of the plasma and the concentration of ozone produced. This type of granite as barrier that produces light intensity, plasma voltage, discharge current and the resulting ozone concentration is higher than the ceramic type. The peak voltage for DBD with barrier G1 is higher than for other barriers.

5. Acknowledgment

We thank to LPPM Universitas Riau for the financial support through Penelitian Inovasi dan Percepatan Hilirisasi year : 2021.

6. References

[1]. Kogelschatz, U. Dielectric-barrier Discharges: Their History, Discharge Physics, and Industrial Applications. Plasma Chem. Plasma Process. 2003, 23, 1–46. [CrossRef]
[2]. Bernhardt, T.; Semmler, M.L.; Schäfer, M.; Bekeschus, S.; Emmert, S.; Boeckmann, L. Plasma Medicine: Applications of Cold Atmospheric Pressure Plasma in Dermatology. Oxidative Med. Cell. Longev. 2019, 2019, 1–10. [CrossRef] [PubMed]
[3]. Weltmann, K.-D.; von Woedtke, T. Plasma medicine – Current state of research and medical application. Plasma Phys. Control. Fusion 2017, 59, 014031. [CrossRef]

[4]. Foster, J.E. Plasma-based water purification: Challenges and prospects for the future. Phys. Plasmas 2017, 24, 055501. [CrossRef]
[5]. Gabriele Neretti, Mattia Ricco. Self-Tuning High-Voltage and High-Frequency Sinusoidal Power Supply for Dielectric Barrier Discharge Plasma Generation. Electronics 2019, 8(10), 1137; https://doi.org/10.3390/electronics8101137
[6]. Wagner, H.-E.; Brandenburg, R.; Kozlov, K.; Sonnenfeld, A.; Michel, P.; Behnke, J. The barrier discharge: basic properties and applications to surface treatment. Vacuum 2003, 71, 417–436. [CrossRef]
[7]. Vandenbroucke, A.M.; Morent, R.; De Geyter, N.; Leys, C. Non-thermal plasmas for non-catalytic and catalytic VOC abatement. J. Hazard. Mater. 2011, 195, 30–54. [CrossRef] [PubMed]
[8]. J. Ouyang, B. Li, F. He, and D. Dai, Atmospheric pressure self-organized filaments in dielectric barrier discharge excited by a modulated sinusoidal voltage. Plasma Sci. Technol. 20, 103002 (2018).
[9]. W. Liu, L. Dong, Y. Wang, X. Zhang, and Y. Pan. Formation mechanism of dot-line square superlattice pattern in dielectric barrier discharge. Phys. Plasmas 21, 113504 (2014).
[10]. L. Yang, Z. Liu, Z. Mao, S. Li, and Q. Chen. Formation and characteristics of patterns in atmospheric-pressure radio-frequency dielectric barrier discharge plasma. Jpn. J. Appl. Phys., Part 1 56, 01AC02 (2017).
[11]. L. Dong, Y. He, W. Liu, R. Gao, H. Wang, and H. Zhao. Hexagon and square patterned air discharges. Appl. Phys. Lett. 90, 031504 (2007).
[12]. Kettlitz M, H Hoft. Hoder T,Reuter S,Weltmann K-D and Brandenburg R. On the spatio-temporal development of pulsed barrier discharges: influence of duty cycle variation 2012 J. Phys. D: Appl. Phys. 45 245201
[13]. Williamson J,Trump D,Bletzinger P and Ganguly B. Comparison of high-voltage ac and pulsed operation of a surface dielectric barrier discharge. 2006 J. Phys. D: Appl. Phys. 39 4400–6
[14]. M Kettlitz, H Hoft, T Hoder, K-D Weltmann and R Brandenburg. Comparison of sinusoidal and pulsed-operated dielectric barrier discharges in an O 2 /N 2 mixture at atmospheric pressure. 2013. Plasma Sources Science and Technology 22(2):025003 DOI:10.1088/0963-0252/22/2/025003
[15]. Fri Murdiya, Febrizal and Amun Amri 2017 The performance of surface barrier discharge in magnetic field driven by half bridge series resonance converter, Journal of Mechatronics, Electrical Power, and Vehicular Technology 8 (2) 95-102 doi: 10.14203/j.mev.2017.v8.95-102
[16]. Fri Murdiya, Febrizal Ujang, and Amun Amri 2020 The Effect of The Magnetic Field on An Ozone Generator Fed by A Non-Sinusoidal Resonance Inverter International Journal on Electrical Engineering and Informatics 12(2) *DOI: 10.15676/ijeei.2020.12.2.12*.
[17]. *Plasma Chemistry*. New York: Cambridge Univ. Press, 2008, pp. 157–159.
[18]. J. S. Townsend, “The conductivity produced in gases by the motion of negatively-charged ions,” *Nature*, vol. 62, no. 1606, pp. 340–341, Aug. 1900.
[19]. H. Luo, Z. Liang, B. Lv, X. Wang, Z. Guan, and L. Wang, “Observa- tion of the transition from a Townsend discharge to a glow discharge in helium at atmospheric pressure,” *Appl. Phys. Lett.*, vol. 91, no. 22, pp. 221504-1–221504-3, Nov. 2007.
[20]. R. Brandenburg, Z. Navrátil, J. Jánsky, P. St’ahel, D. Trunec, and H.-E. Wagner, “The transition between different modes of barrier dis- charges at atmospheric pressure,” *J. Phys. D, Appl. Phys.*, vol. 42, no. 8, pp. 085208-1–085208-10, Apr. 2009.
[21]. N. Gherardi, S. Martin, and F. Massines, “A new approach to SiO_2 deposit using a $N_2{-}SiH_4{-}N_2O$ glow dielectric barrier-controlled discharge at atmospheric pressure,” *J. Phys. D, Appl. Phys.*, vol. 33, no. 19, pp. L104–L108, Oct. 2000.

Fri Murdiya was born on February, 5th, 1980 in Jambi. He graduated his Bachelor Degree from Departement of Electrical Engineering Universitas Sumatera Utara in 2003. He also graduated his Master Degree from Institut Teknologi Bandung in 2009. He got an overseas scholarship for a doctoral program at Kanazawa Institute of Technology in Japan in 2012 and completed his studies in 2015. He is interested in high voltage plasma technology, high voltage engineering and application of high voltage engineering in many areas. He is active in international conference for high voltage engineering and electrical engineering. He is IEEE member since 2012.

Ericko Hardiwika was born May 30, 1996 in Minas, Pekanbaru-Riau. He completed his elementary school (SDN003 Minas Barat) in 2008, and then at MTsN Muara Fajar in 2011. He also graduated at SMAN 1 Minas in 2014 and finally he has completed his undergraduate education, Bachelor of Electrical Engineering at the Universitas Riau in 2020, with a concentration in Power System. He is interested in dielectric barrier discharge, ozone generator and high voltage engineering.

Muhammad Rafi Epafras was born in Dumai, Riau Province on December 23rd, 1997, is the 2nd child of the couple Amrizal and Wentri. He completed his education at State Elementary School (SDN) 008 Dumai-Riau in 2010, then graduated at SMPN 3 DUMAI-RIAU in 2013, then at SMAN 1 DumaI-Riau from 2013 to 2016 and finally he has completed his undergraduate education, Bachelor of Electrical Engineering at the Universitas Riau in 2021, with a concentration in Power System. The author is also part of the Assistant Measurement Laboratory, Basic Electronics Laboratory, Electrical Circuits Laboratory for 4 years at the University of Riau.

Faisal Setiawan was born in Biaro, Agam Regency, West Sumatra on September 15th, 1997, he is the 3rd child of Merizal Efendi and Sestri Yenni. He completed his education at the State Elementary School (SDN) 07 Mandau-Riau in 2010, then graduated at the State Junior High School (SMPN) 01 Mandau-Riau in 2013. Then at SMAN 01 Mandau-Riau from 2013 to 2016, and finally he has completed his undergraduate education, Bachelor of Electrical Engineering at the Universitas Riau in 2021, with a concentration in Power System. The author is also an Assistant for the Protection Laboratory and the Medium Voltage Laboratory.

Firdaus was born on May, 10, 1977 in Pekanbaru. He graduated his Bachelor Degree from Departement of Electrical Engineering Universitas Sriwijaya in 2003. He also graduated his Master Degree from Universitas Indonesia in 2007. He is interested in microcontroller, Io, sensor and tranducer, and electronic circuit. He is IEEE member since 2017.

Amir Hamzah was born on July, 5th, 1975 in Pekanbaru. He graduated his Bachelor Degree from Departement of Electrical Engineering Universitas Sumatera Utara in 1999. He also graduated his Master Degree from Institut Teknologi Bandung in 2008. He is interested in power electronic circuit, electric machines and renewable energy. He is active in international conference. He is IEEE member since 2017.

Febrizal Ujang was born on February, 22th, 1978 in Bengkalis. He graduated his Bachelor Degree from Departement of Electrical Engineering Universitas Sumatera Utara in 2002. He also graduated his Master Degree from Institute Teknologi Bandung in 2009. Currently he is receiving a scholarship for a doctoral program at the University of Indonesia in Depok. He is interested in photonics technology and telecommunication engineering. He is active in international conference for telecommunication engineering and electrical engineering. He is IEEE member since 2017.